Biochemical and Biophysical Research Communications 431 (2013) 169–175

Contents lists available at SciVerse ScienceDirect

Biochemical and Biophysical Research Communications

journal homepage: www.elsevier.com/locate/ybbrc

Fe-SOD cooperates with Nutlin3 to selectively inhibit cancer cells in *vitro* and in *vivo*

Yong Qin, Wei Dai, Yu Wang, Xing-Guo Gong *, Min Lu *

Institute of Biochemistry, College of Life Sciences, Zhejiang University, Hangzhou, China

ARTICLE INFO

Article history:
Received 26 December 2012
Available online 9 January 2013

Keywords:
Cancer targeting
ROS
Fe-SOD
Nutlin3
Synergistic inhibition

ABSTRACT

Nutlin3, a non-genotoxic agonist of p53, is currently in phase II clinical trials for cancer treatment. However, its effects on normal tissues and cell types remain largely to be determined. Drugs that can selectively target cancer cells as well as cooperate with the p53 pathway are thus greatly needed. Iron-superoxide dismutase (Fe-SOD) is a potential candidate as it selectively targets cancer cells by eliminating the abnormally high levels of reactive oxygen species (ROS) in cancer cells; it also inhibits cancer cell growth by induction of p27. Here, we show evidence that modulating redox and ROS homeostasis cooperates with Nutlin3 to selectively inhibit cancer cells in *vitro* and in *vivo*. Co-treatment of Fe-SOD and Nutlin3 showed synergistic inhibition on cancer cells in *vitro*, and the induction of p27 appeared to be involved. No effects were observed on normal cells. In addition, such co-treatment further exhibited synergistic inhibition on tumor growth in *vivo* in a murine B16 xenograft model, while the individual treatments only achieved very limited inhibition. Thus, Fe-SOD cooperated with Nutlin3 to selectively inhibit cancer cells in *vitro* and in *vivo*.

1. Introduction

Functional inactivation of the p53 tumor suppressor pathway is believed to be involved in most human cancers. The p53 gene is directly mutated in approximately 50% of human malignancies, whereas tumors retaining wild-type p53 contain other genetic aberrations that inhibit the tumor suppressor function of p53 [1,2]. Thus, reactivation of p53 shows promise for treating the 50% of cancers that express wild-type p53.

To restore the tumor suppressor function of p53 in human tumors that express wild-type p53, a small-molecule p53 agonist, Nutlin3, has been developed and tested in Phase II clinical trials [3]. Nutlin3 suppresses tumor growth by disrupting mdm2 and p53 binding, thus preventing p53 degradation. Despite promising effects of Nutlin3 on p53 induction in laboratory studies and initial clinic treatments, Nutlin3 alone only caused modest reactivation of p53 in some wild-type p53-expressing cells such as malignant melanomas [4,5]. Like most other drugs employed in cancer therapy, it is unlikely that Nutlin3 will be used as a monotherapy. In this respect, Nutlin-3 shows a synergistic cytotoxic effect when used in combination with TRAIL or bortezomib [6,7]. In addition to inefficiently suppressing the growth of some malignant cells, Nutlin3 also induces p53 in normal tissues and cell types with intact mdm2-p53 pathways, and its effects on normal tissues and cell types remain largely to be determined. Currently, these issues have not been addressed in any reported studies. Thus, drugs that can selectively target cancer cells as well as cooperate with Nutlin3 will greatly improve the success of Nutlin3 therapy.

Selectively targeting cancer cells has been met with varying successes. Theoretically, targeting strategies are based on the differences between cancer and normal cells, including the expression of oncogenes that are abnormally activated and non-oncogenes that perform extremely vital functions in cancer cells. Selectively targeting the activated oncoprotein BRAF V600E in melanomas has been successfully achieved in laboratory studies, as well as in preclinical studies [8]. Targeting non-oncogenes that are extremely vital for cancer cells has also been suggested. During malignant transformation of cells, oxidative stress, replicative stress, metabolic and proteotoxic stress, and stress from DNA damage are frequently enhanced [9]. Among these, oxidative stress is strikingly enhanced. Normal cells have low basal levels of ROS [9–11], and therefore a limited reliance on the ROS stress-response pathway, whereas cancer cells have high levels of ROS [10] and thus might be expected to have a higher reliance on the ROS stress-response pathway [9,11]. Targeting cancer cells by ROS-mediated mechanisms has been extensively studied [11]. While increased ROS levels lead to damage on mitochondrial membranes, release of cytochrome *c* from mitochondria and consequent apoptosis [12], decreased ROS levels lead to dephosphorylation of AKT, upregulation of p27 and consequently cell growth arrest [13,14]. Thus, Fe-SOD could be a candidate for targeting cancer cells because it can efficiently eliminate the abnormally high levels of ROS in cancer cells, and modulate redox and ROS homeostasis [13].

* Corresponding authors. Address: Room 345, Institute of Biochemistry, College of Life Sciences, Zhejiang University, Hangzhou 310058, China. Fax: +86 57188206549.
E-mail address: sc9910@hotmail.com (M. Lu).

0006-291X/$ - see front matter © 2013 Elsevier Inc. All rights reserved.
http://dx.doi.org/10.1016/j.bbrc.2013.01.001

Here, we provide evidence that modulating redox and ROS homeostasis cooperates with Nutlin3 to selectively inhibit cancer cells *in vitro* and *in vivo*. Co-treatment with Fe-SOD and Nutlin3 showed synergistic inhibition on cancer cells *in vitro*, in which induction of p27 was involved. However, normal cells remained unaffected. In addition, such co-treatment further exhibited synergistic inhibition on tumor growth *in vivo* in a murine B16 xenograft model, while the individual treatments only achieved very limited inhibition. We thus put forward a potential approach using Fe-SOD to cooperate with Nutlin3 to overcome the disadvantages of Nutlin3 for the clinical treatment of cancer.

2. Materials and methods

2.1. Antibodies, chemicals, and cell lines

Primary antibodies were purchased from these companies: Santa Cruz (AKT, p-AKT (Thr308), p21, p27, Bax), Abcam (tubulin, PIG3), Cell Signaling (cleaved Caspase-3, total Caspase-3, PUMA), and Vector labs (p53). The ROS probe dihydrorhodamine123 (DHR123) was purchased from Molecular Probes. Nutlin3 and Fe-SOD were obtained from Sigma. Twelve cell lines were available in our institute.

2.2. Cellular ROS determination

Levels of cellular ROS were determined using DHR123. Briefly, 0.5×10^6 cells were collected and incubated with 0.25 μM DHR123 for 15 min at 37 °C. After two washes, cells were stored on ice until FACS analysis.

2.3. Cell proliferation assay

A suspension of 4×10^3 cells was pre-seeded in triplicate to each well of 96-well plates for 24 h. Liposome-encapsulated Fe-SOD (Lip-SOD) and Nutlin3 were added to each well. After 72 h, 20 μl MTT (5 mg/ml) was added to each well followed by standard MTT assay.

2.4. Fe-SOD FITC conjugation and liposome encapsulation

Fe-SOD was encapsulated in liposomes as described previously [14]. For xenograft experiments, Fe-SOD was conjugated with FITC according to the manufacturer's protocol (F-6434, Invitrogen) before liposome encapsulation.

2.5. p53 knock-down

p53 siRNA (M-040642-02-0005, Dharmacon) was transfected into B16 cells using DharmaFECT 1 Transfection Reagent kit. Protein levels were determined by immunoblotting.

2.6. FACS analysis and colony formation assay

Pre-seeded cells were digested, transfected with siRNA, and seeded on 6-well plates for 48 h. Cells were treated with DMSO, Lip-SOD, Nutlin3, or combinations for 72 h. The treated cells were collected and used for the following two analyses. For cell cycle analysis, cells were fixed in 70% ethanol at 4 °C for 12 h and then stained by 0.05 mg/ml PI for 30 min at room temperature. The DNA content was determined by FACS analysis. For colony formation assays, 1000 cells/well were seeded in 6-well plates and kept in culture for 12 days.

2.7. Xenograft assay

Treated or untreated B16 cells (1×10^6) were subcutaneously injected into the flanks of 8 week-old female C57BL/6 mice at day 1. At day 3 or day 7, 40 mg/kg Nutlin3 or 1×10^5 U/kg Lip-SOD were intraperitoneally injected either individually or in combination every 2 days. Tumor size was measured every 2 days with a vernier caliper. Tumor volumes were calculated using the following formula: (L∗W∗W)/2, in which L represents the large diameter of the tumor, and W represents the small diameter. On day 13, all the animals were sacrificed and tumors were weighted.

3. Results

3.1. Lip-SOD selectively inhibits cancer cells independent of p53 status

During malignant transformation in cells, cellular stresses including oxidative stress are enhanced. ROS-related pathways could be targeted for cancer treatment. We investigated cellular ROS levels in a panel of normal cell lines and cancer cell lines. Twelve cell lines exhibiting distinct malignancy and p53 status were collected and subjected to ROS determination. Relatively low ROS levels were observed in the normal or poorly malignant cells, while much higher ROS levels were universally observed in all of the malignant cancer cells (Fig. 1A). Specifically, immortalized highly malignant transformed MEFs showed significantly higher ROS levels than primary MEFs. The same trend was observed in HaCaT keratinocyte cells and the malignant counterpart A431 cells (Fig. 1B). In addition, ROS levels were not associated with p53 status in the 12 cell lines examined (Fig. 1A).

We tested the sensitivity of the 12 cell lines exposed to disturbed ROS homeostasis. Fe-SOD was used to eliminate the superoxide anions, which are generated in the mitochondria and are the primary origin of cellular ROS. Lip-SOD was shown to efficiently penetrate cellular membranes and decrease cellular ROS levels [14]. 50–100 U/ml Lip-SOD universally showed cell growth inhibition on all 12 cell lines, although IC_{50} values varied. Strikingly, the primary and non-malignant cells that contain low ROS levels showed much higher resistance to Lip-SOD treatment, while the cancer cells with high ROS levels were more sensitive to Lip-SOD treatment (Fig. 1C). Fe-SOD showed higher growth inhibition on the cancer cells with high ROS levels.

Taken together, cancer cells universally possessed much higher cellular ROS levels and were more sensitive to Fe-SOD treatment.

3.2. Fe-SOD cooperates with Nutlin3 to selectively inhibit cancer cells by induction of p27 in vitro

We previously showed that Fe-SOD inhibited cancer cell growth by dephosphorylating AKT and upregulating p27 [13,14]. p53 is suggested to display synergy with p27 in regards to tumor suppression [15,16]. We thus determined whether Lip-SOD could confer Nutlin3 tumor selectivity and synergistically inhibit cancer cell growth.

Consistent with the growth inhibitory role of p53, 2 μM Nutlin3 efficiently inhibited cell growth by 50% in 5/7 of cancer cell lines that express wild-type p53, but not in any of the cells containing mutant p53 (Fig. 2A). However, two wild-type p53-containing cell lines, A375M and B16, showed considerable resistance to Nutlin3. It is not clear as to why some cells, specifically melanoma cells, were resistant to Nutlin3 treatment even though high levels of p53 were induced (Fig. 3A). Nutlin3 also induced p53 and partially inhibited cell growth in normal cells (~30% inhibition for 2 μM Nutlin3, ~50% inhibition for 5 μM Nutlin3 in normal MEFs). In addition, it seems that the inhibition achieved by high Nutlin3

A

	Description	Malignancy	ROS level	p53 status
MEFs (mouse)	Embryonic Fibroblasts	Normal cells	+	WT
L929 (mouse)	Fibrosarcoma	poor	+	WT
HaCaT	Immortalized keratinocyte	Resemble normal keratinocytes	+	Mutant
A431	Keratinocyte	Malignant	+++	Mutant
AGS	Gastric carcinoma	Malignant	++	WT
HepG2	Liver carcinoma	Malignant	+++	WT
MCF7	Breast adenocarcinoma	Malignant	++	WT
SK-MEL-28	Melanoma	Malignant	+++	Mutant
A375P	Melanoma	Malignant (poorly metastatic)	+++	WT
A375M	Melanoma	Malignant (highly metastatic)	+++	WT
B16 (mouse)	Melanoma	Highly malignant	+++	WT
Immortalized MEFs (mouse)	Ras/E1A transformed MEFs	Highly malignant	+++	WT

ROS level +: Mean DHR123 fluorescence intensity < 200;
++: Mean DHR123 fluorescence intensity 200-400;
+++: Mean DHR123 fluorescence intensity > 400.

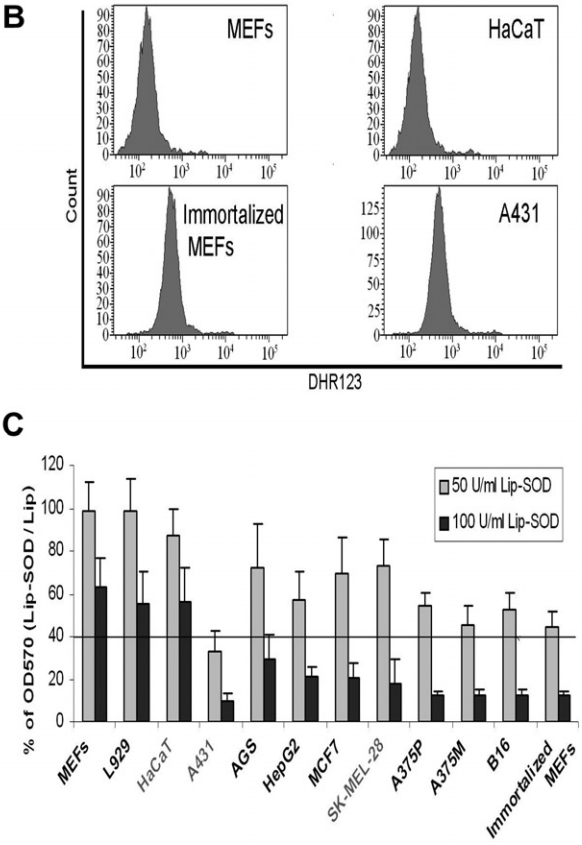

Fig. 1. Lip-SOD selectively inhibits cancer cells independent of p53 status. A. Summary of cellular ROS levels, p53 status, and malignancy in a panel of 12 cell lines examined. B. FACS analysis of DHR123 fluorescence intensity in indicated cell lines. Experiments were conducted on the entire 12 cell line panel, and the representative profiles from 4 indicated cell lines were shown. C. MTT cytotoxicity assays of Lip-SOD on 12 cell lines. 50–100 U/ml Lip-SOD were added for 72 h. Empty liposomes were used as control. A_{570} was then measured after MTT incubation. Cell lines with mutant p53 are shown in gray. Bar graphs are shown by mean ± SD from three independent experiments.

(20 μM) is partially p53-independent as several p53 mutant containing cell lines were also largely inhibited (~80% inhibition for A431, ~70% inhibition for SK-MEL-28). Nutlin3 showed partially growth inhibition on normal cells in *vitro*.

When the panel of cells was co-treated with Lip-SOD and low concentrations of Nutlin3, obvious synergistic inhibition was observed. 2 μM Nutlin3 was enough to inhibit all of the cancer cells expressing wild-type p53 by 70% in the presence of 50 U/ml Lip-SOD (Fig. 2B). In B16 cells, though 50 U/ml Lip-SOD or 2 μM Nutlin3 individually inhibited cell growth less than 50%, the combination treatment inhibited cell growth by ~85%. Most importantly, co-treatment showed selectivity towards cancer cells, and these treatments did not significantly inhibit any of the three normal cell lines (over 70% cells survived). These data demonstrate that Fe-SOD cooperated with Nutlin3 to selectively inhibit growth of cancer cells in *vitro*.

We then aimed to investigate the pathways involved in the synergistic inhibition observed in B16 melanoma cells. Previous studies showed that Fe-SOD inhibited cell growth by dephosphorylating AKT and upregulating p27 [13,14]. p53 is well documented to induce cell apoptosis or cell cycle arrest by activating the transcription of targeted apoptotic genes (including BAX, PIG3, and PUMA) or cell cycle arrest related genes (including p21). Therefore, the levels of these proteins were determined after treatment. As previously observed, AKT dephosphorylation on Thr308 and consequent upregulation of p27 were induced by Lip-SOD treatment (Fig. 3A). However, proteins involved in the p53 pathway including p21, BAX, PIG3, and PUMA as well as an apoptotic marker (cleaved caspase-3) showed limited induction after Lip-SOD treatment. In addition, p53 appeared to not be involved in Lip-SOD-induced pathways as knocking down p53 showed very limited effect on the levels of p-AKT and p27 (Fig. 3A).

While Nutlin3 significantly upregulated the level of a cell cycle related target (p21), Nutlin3 treatment showed a limited effect on apoptosis related targets (BAX and PIG3) and an apoptosis marker (cleaved caspase-3) (Fig. 3A). Nutlin3 significantly upregulated the level of p27, although p27 was not expected to be the direct transcriptional target of p53. When cells were treated with Nutlin3 in presence of Lip-SOD, p27 was induced to a strikingly greater degree. Slight, but detectable, increases in BAX and PIG3 were also observed. These results imply that the synergistic inhibition induced by Nutlin3 and Lip-SOD is largely mediated by a cell cycle arrest-related pathway and partially mediated by apoptosis pathways.

Supporting above conclusion, Lip-SOD treatment induced a significant increase in the proportion of G_1 cells, but not apoptotic cells (determined by percentage of cells containing sub-G_1 DNA content), in B16 cells (Fig. 3B). Nutlin3 treatment induced a significant increase in the proportion of G_1 cells, as well as a detectable increase in apoptotic cells. Interestingly, Lip-SOD and Nutlin3 co-treatment induced both significant increases in the proportion of G_1 cells, as well as apoptotic cells (12% vs. 1.0%). Another striking difference between the Nutlin3 + Lip-SOD group and the control group was a decrease in the proportion of cell in G_2/M (29% vs. 5.9%). These data indicate that enhanced proportion of sub-G_1 and G_1 cells as well as decreased proportion of G_2/M cells were involved in current synergistic inhibition.

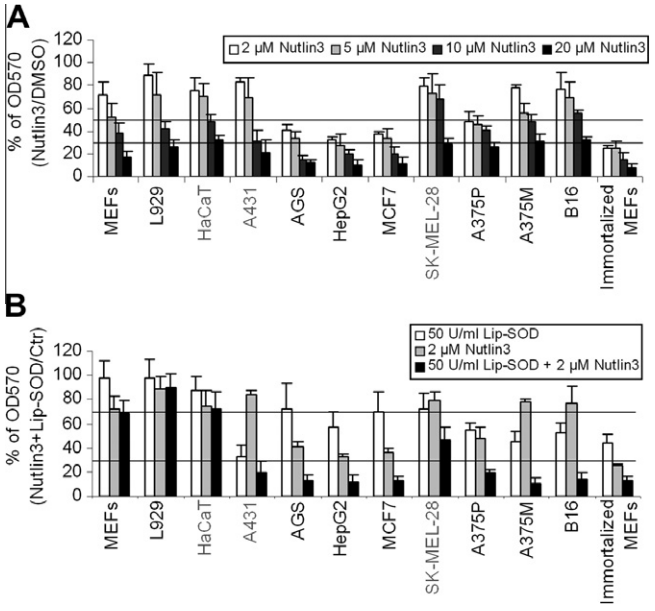

Fig. 2. Fe-SOD cooperates with Nutlin3 to selectively inhibit cancer cells in *vitro*. A. MTT cytotoxicity assays of Nutlin3 on a panel of 12 cell lines. Cells were seeded and 2–20 μM Nutlin3 was added for 72 h. DMSO was used as a control. B. MTT cytotoxicity assays of Lip-SOD and Nutlin3 on a panel of 12 cell lines. Cells were treated with 50 U/ml Lip-SOD + 2 μM Nutlin3 as described above, followed by MTT cytotoxicity assays. Empty liposomes and DMSO (Lip + DMSO) were used as control. In A and B, cell lines with mutant p53 are shown in gray. Bar graphs are shown by mean ± SD from three independent experiments. The bars of the 50 U/ml Lip-SOD group and the 2 μM Nutlin3 group were derived from Figs. 1C and 2A.

3.3. Co-treatment of Fe-SOD and Nutlin3 synergistically inhibits B16 tumor growth in vivo

B16 cells are known to form highly aggressive melanoma tumors *in vivo* in immune competent C57BL/6 syngeneic mice. The synergistic inhibition of B16 cells *in vitro* by Lip-SOD and Nutlin3 co-treatment was validated using B16 xenografts *in vivo*. The tumorigenicity of B16 cells treated *in vitro* with Lip-SOD and Nutlin3 was initially determined using colony formation assays, as well as tumor formation experiments in mice. Interestingly, only 27% of cells treated by Lip-SOD + Nutlin3 formed colonies, although over 50% of cells treated with either Lip-SOD or Nutlin3 formed colonies (Fig. 4A). Consistent with these results, we observed that the weights of tumors derived from mice injected with B16 cells pretreated with Lip-SOD, Nutlin3 or Lip-SOD + Nutlin3 were approximately 54%, 61% or 21% of those derived from the DMSO group (Fig. 4B), respectively. These observations indicate that *in vitro* co-treatment of Lip-SOD and Nutlin3 confers less colony formation and reduced tumorigenicity in B16 cells.

The ability of Lip-SOD + Nutlin3 cotreatment to inhibit B16 melanoma growth *in vivo* was further tested by inoculating untreated B16 cells into C57BL/6 mice followed by intraperitoneally administration of Lip-SOD, Nutlin3 or Lip-SOD + Nutlin3 on day 3 (after cells initially settle down, Fig. 4C) or day 7 (after tumors become visible, Fig. 4D). Drugs were administered every 2 days as indicated. To probe the exogenously introduced Fe-SOD, Fe-SOD was labeled with FITC before liposome encapsulation (Lip-SOD-FITC). Treatment with Lip-SOD-FITC + Nutlin3 from day 3 or day 7 suppressed the tumor weight of B16 melanomas by 76% or 70% compared to DMSO, respectively. Administration of Lip-SOD-FITC

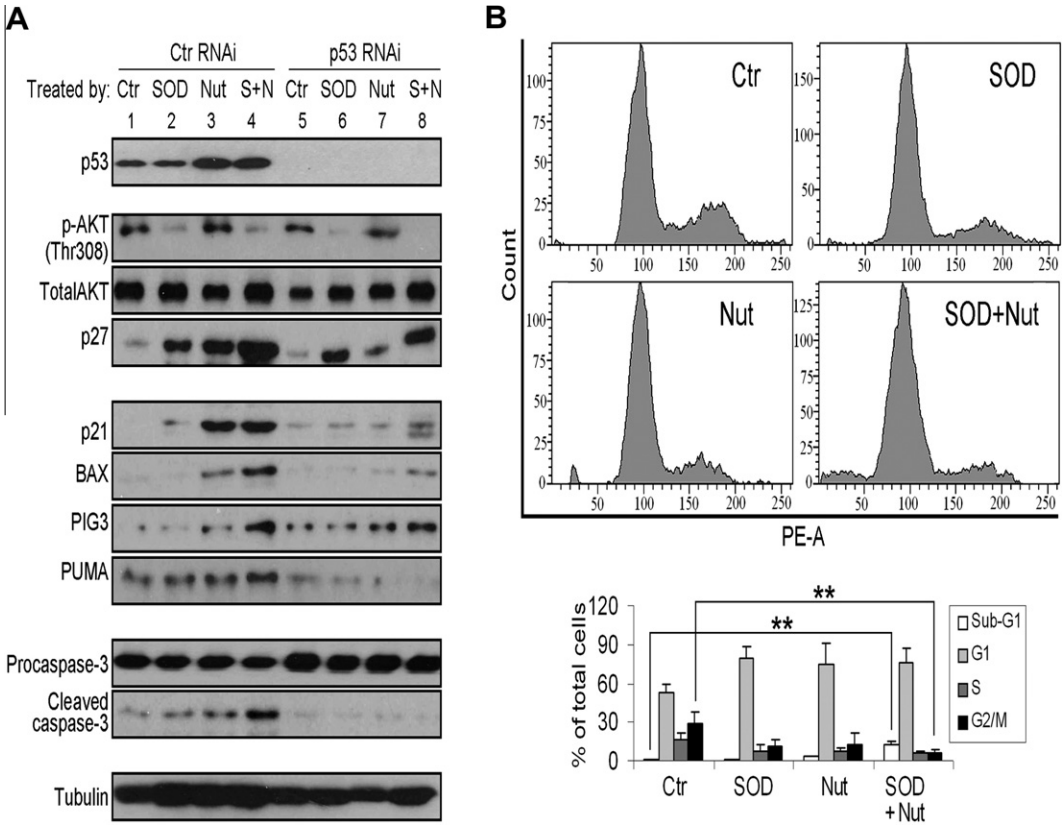

Fig. 3. Induction of p27 and cell cycle arrest are involved in cooperation between Fe-SOD and Nutlin3. A. Synergistic induction of p27 by Lip-SOD and Nutlin3. p53 siRNA was transfected into B16 cells for 48 h. Cells were then treated for 72 h (SOD: 50 U/ml Lip-SOD; Nut: 2 μM Nutlin3; S + N: 50 U/ml Lip-SOD + 2 μM Nutlin3). Protein levels were determined by immunoblotting. B. FACS analysis of the cell cycle distribution of B16 cells after treatment. Left panel shows a representative cell cycle profile of B16 cells after treatment. Right bar graph shows the percentage of treated cells in various cell phases. Graphs are shown as the mean ± SD from three independent experiments (**$p < 0.01$).

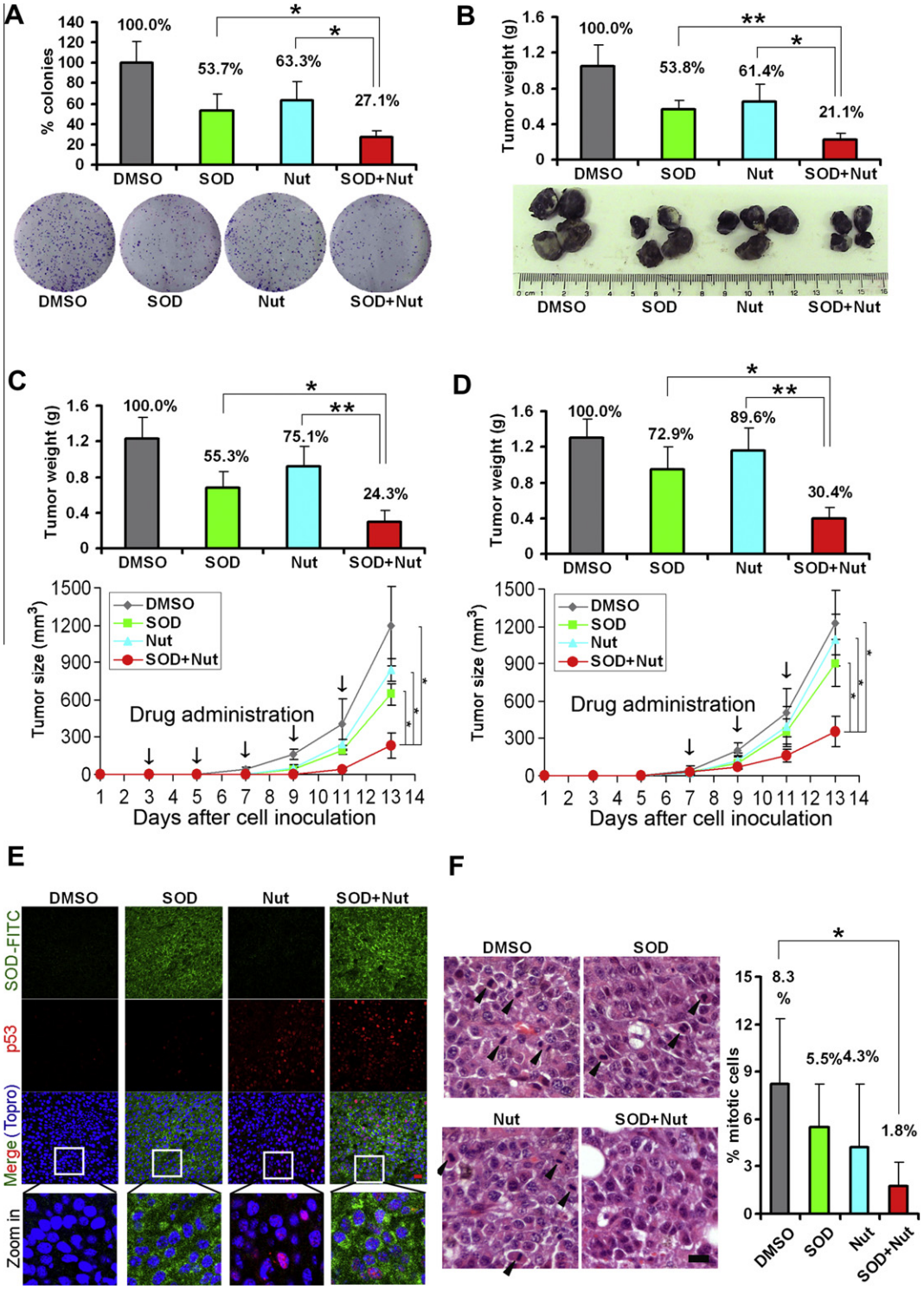

Fig. 4. Fe-SOD and Nutlin3 synergistically inhibit B16 tumor growth in *vivo*. A. B16 cells were treated with Lip-SOD (SOD), Nutlin3 (Nut) or a combination. Bar graph shows the percentages of treated cells that formed colonies. Bar graphs (mean ± SD) were derived from three independent experiments ($^{*}p < 0.05$). B. B16 cells were treated as indicated and subcutaneously injected into the flanks of mice on day 1. Mice were fed and tumors were isolated on day 13. Bar graphs (mean ± SD) show the tumor weight in each group ($^{*}p < 0.05$, $^{**}p < 0.01$, $n = 4$). C. Untreated B16 cells were subcutaneously injected into the flanks of mice on day 1. Drugs were intraperitoneally injected and tumor size was measured every 2 days beginning on day 3. Bar graphs are shown as the mean ± SD ($^{*}p < 0.05$, $^{**}p < 0.01$, $n = 4$). D. Untreated B16 cells were subcutaneously injected into the flanks of mice and treated as described in C with the exception that the drug administration began on day 7. E. Example of fluorescence signals of Lip-SOD and p53 in tumor sections derived from C. Lip-SOD signals were probed by conjugated FITC (green) and p53 signals were probed by p53 antibody staining (CM5, red). Nuclei were probed by Topro (blue). Bar = 20 μm. F. Left panel, representative H and E staining of B16 tumor sections derived from C. Cells in mitosis were marked with black arrowheads. Bar = 20 μm. Right panel, the number of cells in mitosis was counted from 3 independent tumors and a percentage was calculated. At least 200 cells were counted in each section. Bar graphs are shown by mean ± SD ($^{*}p < 0.05$). (For interpretation of the references to color in this figure legend, the reader is referred to the web version of this article.)

alone from day 3 or day 7 suppressed B16 melanoma growth by 45% or 27%, while administration of Nutlin3 alone from day 3 or day 7 suppressed B16 melanoma growth by 25% or 10%, respectively (Fig. 4C and D). Altogether, these findings demonstrate that synergistic inhibition of B16 melanoma cells *in vivo* was achieved by co-treatment with Lip-SOD-FITC and Nutlin3 at both time points.

To further confirm that the synergistic inhibition is indeed caused by introduced Fe-SOD-FITC and Nutlin3-induced p53, the levels of Fe-SOD-FITC and p53 were determined in isolated B16 tumor sections. In the DMSO group, both FITC and p53 were almost undetectable. In B16 tumors treated with Lip-SOD-FITC, cytoplasmic SOD-FITC signal was predominant, but p53 was not observed. Nutlin3 treatment induced nuclear p53 expression. Treatment with Lip-SOD-FITC + Nutlin3 resulted in detectable cytoplasmic SOD-FITC signal and an increase in nuclear p53 (Fig. 4E). These data demonstrate that observed synergistic inhibition was associated with increased cytoplasmic SOD level and nuclear p53 level.

In addition, we observed a significantly smaller proportion of mitotic cells in the Lip-SOD + Nutlin3-treated B16 tumors when compared to control tumors (1.8% vs. 8.3%, Fig. 4F). Cell cycle arrest might be involved in the synergistic inhibition of B16 xenografts.

4. Discussion

Reactive oxygen species (ROS) are chemically reactive molecules that are constantly generated and eliminated during diverse biological and cellular reactions, and ROS are known to serve dual roles as both deleterious and beneficial species [17]. Unregulated and redundant ROS are highly toxic to cells due to the peroxidative activity towards biological constituents. Small molecules that alter ROS levels, such as buthionine sulphoximine, have been used for cancer treatment [18]. Huang et al. used estrogen derivatives to enhance ROS levels and selectively kill human leukemia cells but not normal lymphocytes [12]. An increasing body of evidence indicates that cancer cells exhibit increased intrinsic ROS levels compared with normal cells, due in part to oncogenic stimulation, alterations in metabolic activity, and mitochondrial malfunction, and increased ROS levels may stimulate cellular proliferation, promote mutations and genetic instability, and alter cellular sensitivity to anticancer agents [17]. Several studies have confirmed that elimination of excessive ROS by chemical or enzymatic antioxidants decreases the tumorigenicity of tumor cells [19,20]. Thus, in addition to modulating redox by enhancing oxidative stress, reducing oxidative stress may be another potential strategy to selectively target cancer cells.

Despite the successful universal induction of p53, three disadvantages of Nutlin3 were identified in current studies. First, some cancer cell lines were resistant to Nutlin3 despite high induction of p53. This result is consistent with other studies [4,5]. Second, Nutlin3 also induced p53 and partially inhibited cell growth in normal cells. Third, treatment with high concentrations of Nutlin3 caused non-specific growth inhibition. In the current studies, Fe-SOD, a compound that can selectively target cancer cells, was used to overcome the above three disadvantages, and a selective and synergistic inhibition of melanoma cells was observed *in vitro* and *in vivo*.

Though the detailed pathways involved in the current synergistic inhibition remain unknown, the cooperation of Fe-SOD and p53 in synergistically inducing p27 is suggested to be involved. In contrast, the apoptotic pathways are suggested to be weakly involved. Mechanistically, p27 is reported to be involved in the AKT pathway [21]. Downregulation of phosphorylated AKT and upregulation of p27 protein level in Fe-SOD-treated cancer cells were also observed in our previous studies [13,14]. However, the involvement of p27 in the p53 pathway is not fully realized. While p27 is functionally similar to the tumor suppressor p21, p21 is generally reported to be a transcriptional target of p53, and p27 is not directly subjected to p53 transcriptional regulation. However, at least two groups have reported a positive association between p27 and p53 protein levels, and both groups observed a downregulation of p27 in p53 knocking out mice, which was largely achieved at the post-transcriptional level [15,16]. Thus, p27 might be subjected to regulation by p53 at the post-transcriptional level. This is consistent with the current observation that induction of p27 by Fe-SOD is strikingly amplified in the presence of Nutlin3.

Overall, we show that Fe-SOD cooperates with Nutlin3 to overcome some disadvantages of Nutlin3 treatment. Cancer cells were selectively targeted and synergistically suppressed by co-treatment of Fe-SOD and Nutlin3. Noticeably, p27 was synergistically induced by co-treatment, which might contribute to the observed synergistic suppression of B16 melanoma cells.

Acknowledgments

We thank Mr. David for his comments on the manuscript. This work was supported by grant 30900760 from the National Natural Science Foundation of China (project number J20091073).

References

[1] D.P. Lane, Cancer. p53, guardian of the genome, Nature 358 (1992) 15–16.
[2] P. Hainaut, M. Hollstein, P53 and human cancer: the first ten thousand mutations, Adv. Cancer Res. 77 (2000) 81–137.
[3] B.T. Vu, L. Vassilev, Small-molecule inhibitors of the p53-MDM2 interaction, Curr. Top. Microbiol. Immunol. 348 (2011) 151–172.
[4] J. de Lange, L.V. Ly, K. Lodder, M. Verlaan-de Vries, A.F. Teunisse, M.J. Jager, A.G. Jochemsen, Synergistic growth inhibition based on small-molecule p53 activation as treatment for intraocular melanoma, Oncogene (2011) 1105–1116.
[5] Z. Ji, C.N. Njauw, M. Taylor, V. Neel, K.T. Flaherty, H. Tsao, p53 rescue through HDM2 antagonism suppresses melanoma growth and potentiates MEK inhibition, J. Invest. Dermatol. (2011) 356–364.
[6] T. Hori, T. Kondo, M. Kanamori, Y. Tabuchi, R. Ogawa, Q.L. Zhao, K. Ahmed, T. Yasuda, S. Seki, K. Suzuki, T. Kimura, Nutlin-3 enhances tumor necrosis factor-related apoptosis-inducing ligand (TRAIL)-induced apoptosis through up-regulation of death receptor 5 (DR5) in human sarcoma HOS cells and human colon cancer HCT116 cells, Cancer Lett. 287 (2010) 98–108.
[7] L. Jin, Y. Tabe, K. Kojima, Y. Zhou, S. Pittaluga, M. Konopleva, T. Miida, M. Raffeld, MDM2 antagonist Nutlin-3 enhances bortezomib-mediated mitochondrial apoptosis in TP53-mutated mantle cell lymphoma, Cancer Lett. 299 (2010) 161–170.
[8] H. Yang, B. Higgins, K. Kolinsky, K. Packman, Z. Go, R. Iyer, S. Kolis, S. Zhao, R. Lee, J.F. Grippo, K. Schostack, M.E. Simcox, D. Heimbrook, G. Bollag, F. Su, RG7204 (PLX4032), a selective BRAFV600E inhibitor, displays potent antitumor activity in preclinical melanoma models, Cancer Res. 70 (2010) 5518–5527.
[9] J. Luo, N.L. Solimini, S.J. Elledge, Principles of cancer therapy: oncogene and non-oncogene addiction, Cell 136 (2009) 823–837.
[10] M. Diehn, R.W. Cho, N.A. Lobo, T. Kalisky, M.J. Dorie, A.N. Kulp, D. Qian, J.S. Lam, L.E. Ailles, M. Wong, B. Joshua, M.J. Kaplan, I. Wapnir, F.M. Dirbas, G. Somlo, C. Garberoglio, B. Paz, J. Shen, S.K. Lau, S.R. Quake, J.M. Brown, I.L. Weissman, M.F. Clarke, Association of reactive oxygen species levels and radioresistance in cancer stem cells, Nature 458 (2009) 780–783.
[11] D. Trachootham, J. Alexandre, P. Huang, Targeting cancer cells by ROS-mediated mechanisms: a radical therapeutic approach?, Nat Rev. Drug Discovery 8 (2009) 579–591.
[12] P. Huang, L. Feng, E.A. Oldham, M.J. Keating, W. Plunkett, Superoxide dismutase as a target for the selective killing of cancer cells, Nature 407 (2000) 390–395.
[13] M. Lu, X. Gong, Y. Lu, J. Guo, C. Wang, Y. Pan, Molecular cloning and functional characterization of a cell-permeable superoxide dismutase targeted to lung adenocarcinoma cells. Inhibition cell proliferation through the Akt/p27kip1 pathway, J. Biol. Chem. 281 (2006) 13620–13627.
[14] M. Lu, C.S. Bi, X.G. Gong, H.M. Chen, X.H. Sheng, T.L. Deng, K.D. Xu, Anti-proliferative effects of recombinant iron superoxide dismutase on HepG2 cells via a redox-dependent PI3k/Akt pathway, Appl. Microbiol. Biotechnol. 76 (2007) 193–201.
[15] P. Casalini, M.V. Iorio, V. Berno, A. Bergamaschi, A.L. Borresen Dale, P. Gasparini, R. Orlandi, B. Casati, E. Tagliabue, S. Menard, Relationship between p53 and p27 expression following HER2 signaling, Breast 16 (2007) 597–605.

[16] J. Philipp-Staheli, K.H. Kim, D. Liggitt, K.E. Gurley, G. Longton, C.J. Kemp, Distinct roles for p53, p27Kip1, and p21Cip1 during tumor development, Oncogene 23 (2004) 905–913.

[17] H. Pelicano, D. Carney, P. Huang, ROS stress in cancer cells and therapeutic implications, Drug Resist. Update 7 (2004) 97–110.

[18] P.T. Schumacker, Reactive oxygen species in cancer cells: live by the sword, die by the sword, Cancer Cell 10 (2006) 175–176.

[19] Y. Zhang, W. Zhao, H.J. Zhang, F.E. Domann, L.W. Oberley, Overexpression of copper zinc superoxide dismutase suppresses human glioma cell growth, Cancer Res. 62 (2002) 1205–1212.

[20] M. Valko, C.J. Rhodes, J. Moncol, M. Izakovic, M. Mazur, Free radicals, metals and antioxidants in oxidative stress-induced cancer, Chem. Biol. Interact. 160 (2006) 1–40.

[21] R.H. Medema, G.J. Kops, J.L. Bos, B.M. Burgering, AFX-like Forkhead transcription factors mediate cell-cycle regulation by Ras and PKB through p27kip1, Nature 404 (2000) 782–787.